

## Article

# Assessing the Efficacy of A Mo<sub>2</sub>C/Peroxydisulfate System for Tertiary Wastewater Treatment: A Study of Losartan Degradation, *E. coli* Inactivation, and Synergistic Effects

Alexandra A. Ioannidi<sup>1</sup>, Maria Vlachodimitropoulou<sup>1</sup>, Zacharias Frontistis<sup>2</sup> , Athanasia Petala<sup>3</sup>, Eleni Koutra<sup>1</sup>, Michael Kornaros<sup>1</sup>  and Dionissios Mantzavinos<sup>1,\*</sup> 

<sup>1</sup> Department of Chemical Engineering, University of Patras, GR-26504 Patras, Greece; alex.ioannidi@chemeng.upatras.gr (A.A.I.); m.vlachodimitropoulou@gmail.com (M.V.); ekoutra@chemeng.upatras.gr (E.K.); kornaros@chemeng.upatras.gr (M.K.)

<sup>2</sup> Department of Chemical Engineering, University of Western Macedonia, GR-50132 Kozani, Greece; zfronistis@uowm.gr

<sup>3</sup> Department of Environment, Ionian University, GR-29100 Zakynthos, Greece; apetala@ionio.gr

\* Correspondence: mantzavinos@chemeng.upatras.gr

**Abstract:** This work examines the use of pristine Mo<sub>2</sub>C as an intriguing sodium persulfate (SPS) activator for the degradation of the drug losartan (LOS). Using 500 mg/L Mo<sub>2</sub>C and 250 mg/L SPS, 500 µg/L LOS was degraded in less than 45 min. LOS decomposition was enhanced in acidic pH, while the apparent kinetic constant decreased with higher LOS concentrations. According to experiments conducted in the presence of scavengers of reactive species, sulfate radicals, hydroxyl radicals, and singlet oxygen participated in LOS oxidation, with the latter being the predominant reactive species. The presence of competitors such as bicarbonate and organic matter reduced the observed efficiency in actual matrices, while, interestingly, the addition of chloride accelerated the degradation rate. The catalyst showed remarkable stability, with complete LOS removal being retained after five sequential experiments. The system was examined for simultaneous LOS decomposition and elimination of *Escherichia coli*. The presence of *E. coli* retarded LOS destruction, resulting in only 30% removal after 3 h, while the system was capable of reducing *E. coli* concentration by 1.23 log. However, in the presence of simulated solar irradiation, *E. coli* was reduced by almost 4 log and LOS was completely degraded in 45 min, revealing a significant synergistic effect of the solar/Mo<sub>2</sub>C/SPS system.

**Keywords:** 2D material; peroxydisulfate; pharmaceutical; pathogen; process synergy; solar irradiation



**Citation:** Ioannidi, A.A.; Vlachodimitropoulou, M.; Frontistis, Z.; Petala, A.; Koutra, E.; Kornaros, M.; Mantzavinos, D. Assessing the Efficacy of A Mo<sub>2</sub>C/Peroxydisulfate System for Tertiary Wastewater Treatment: A Study of Losartan Degradation, *E. coli* Inactivation, and Synergistic Effects. *Catalysts* **2023**, *13*, 1285. <https://doi.org/10.3390/catal13091285>

Academic Editor: Enric Brillas

Received: 9 August 2023

Revised: 3 September 2023

Accepted: 6 September 2023

Published: 8 September 2023



**Copyright:** © 2023 by the authors. Licensee MDPI, Basel, Switzerland. This article is an open access article distributed under the terms and conditions of the Creative Commons Attribution (CC BY) license (<https://creativecommons.org/licenses/by/4.0/>).

## 1. Introduction

Following the “technological revolution”, also known as the second industrial revolution, aquatic environmental pollution escalated due to numerous compounds, the effects of which on aquatic ecosystems and humans were unknown. Only in the last half-century, prompted by the threat of drinking water shortages, did the World Health Organization, in collaboration with nations worldwide, establish detection limits for many substances and heavy metals in aquatic environments that are harmful to all organisms [1,2]. However, industrial, agricultural, and sewage wastewater treatment plants have proven to be inadequate for certain types of pollutants (e.g., pharmaceuticals, endocrine disruptors, and pesticides). Many researchers have detected these in surface and groundwater at extremely low concentrations (ng/L–µg/L) [3]. These micropollutants have been found to be toxic to many microorganisms and may cause metabolic disorders and various types of cancer [3,4].

Antihypertensive drugs, which are widely prescribed each year, are a significant type of pharmaceutical [5,6]. In the United States alone, the number of adults with hypertension was approximately 37 million in 2017 [7,8]. Overconsumption of antihypertensive

medications has resulted in their detection in surface waters, wastewater effluents, and environments like wetlands, rivers, and seawaters, as well as in hospital wastewater. Their concentrations ranged from 0.6 ng/L to 17.7 mg/L [9–16].

Losartan (LOS), an antihypertensive medication, reduces the risk of strokes and heart attacks [17,18]. It has also been proven to be a beneficial agent in preventing kidney damage caused by diabetes [17,18]. However, LOS has been found in effluents at concentrations from 19.7 to 2760 ng/L [17,19], indicating the incomplete degradation of LOS using biological wastewater treatment [20–22]. Also, Cortez et al. [9] noted the occurrence of LOS in a Brazilian coastal region with concentrations reaching up to 32 ng/L. Furthermore, Cortez et al. [9], Ladhari et al. [20], Osorio et al. [21], and Adams et al. [22] revealed that despite LOS's numerous benefits for human health, it can be toxic to various organisms, including humans, fish, crustaceans, algae, *Daphnia magna*, and *Desmodesmus subspicatus*. Its byproducts can be more harmful and persistent than the parent compound (LOS). Thus, there is a pressing need to develop alternative methods to efficiently degrade antihypertensive drugs in aqueous media.

Over the past fifteen years, numerous attempts have been made to replace traditional disinfection processes like ozonation [23–25], chlorination [25,26], and UVC irradiation [25,26] due to the potential carcinogenicity of their byproducts or the increased cost. As a result, many scientists have turned their focus towards advanced oxidation processes (AOPs) to find a technology with high efficiency for degrading micropollutants and eradicating pathogenic microorganisms [27–29].

AOPs include a large set of processes (e.g., photocatalysis, Fenton, electrochemical oxidation, and persulfate activation), all of which share the common characteristic of producing strong reactive species such as hydroxyl radicals ( $\text{HO}^\bullet$ ), superoxide radicals, singlet oxygen, and sulfate radicals ( $\text{SO}_4^{\bullet-}$ ) [30]. Technologies based on persulfate activation have garnered considerable attention from the research community for treating hazardous micropollutants in aquatic environments. Persulfate can be activated by heat, solar irradiation, ultrasound, alkaline conditions, and transition metals to form  $\text{SO}_4^{\bullet-}$  with a redox potential ( $E = 2.5\text{--}3.1$  V) similar to the redox potential of  $\text{HO}^\bullet$  ( $E = 1.8\text{--}2.7$  V) [31]. In addition,  $\text{SO}_4^{\bullet-}$  has advantages over hydroxyl radicals in terms of activity over a large pH range, lifespan, and selectivity [32–34]. Furthermore, in the past decade, heterogeneous persulfate activation has gained interest due to the possible reuse of catalytic materials.

Recently, two-dimensional (2D) materials such as graphene [35] and  $\text{MoS}_2$  [36] have gained recognition in the field of wastewater treatment. Up until now, 2D materials have primarily found applications in renewable and sustainable energy production [36,37] because of their high electrical conductivity, thermal stability, high hardness, and adsorption capacity. Considering that 2D materials are characterized by high electron mobility, they are potential persulfate activators. Bekris et al. [35] showed that graphene is an effective persulfate (SPS) activator for propyl paraben degradation, while Zhou et al. [36] examined the activation of peroxymonosulfate (PMS) and SPS with  $\text{MoS}_2$  for the degradation of carbamazepine. However, an excessive use of  $\text{MoS}_2$  after persulfate activation may lead to sulfuric leaching and the formation of  $\text{H}_2\text{S}$ , which is toxic [38].

Molybdenum carbide ( $\text{Mo}_2\text{C}$ ) can be considered an alternative choice for persulfate activation since Mo is the primary active site in Mo-based materials, and given that  $\text{Mo}_2\text{C}$  has two Mo atoms, there is a high probability of it being more reactive. Additionally, it does not exhibit the drawbacks associated with the use of  $\text{MoS}_2$  [39–41].

The exploration of  $\text{Mo}_2\text{C}$  as a persulfate activator for micropollutant degradation has only recently begun. Yang et al. [38] treated  $\text{Mo}_2\text{C}$  with 5% Cu to enhance its ability to activate PMS for tetracycline degradation, while Chen et al. [31] and Bao et al. [42] synthesized  $\text{Mo}_2\text{Ga}_2\text{C}$  and  $\text{Mo}_2\text{C}/\text{C}$  respectively, to activate PMS for bisphenol A and carbamazepine removal. However, there are no studies that investigate solely the potential of pristine  $\text{Mo}_2\text{C}$  to activate SPS, a less expensive oxidant than PMS, for micropollutant degradation and pathogen disinfection without increasing catalyst preparation costs through material modification.

To date, the oxidation of LOS has been explored through various methods, including electrochemical oxidation, heat-activated persulfate, acoustic cavitation, UV/H<sub>2</sub>O<sub>2</sub>, UV/Fe<sup>2+</sup>/H<sub>2</sub>O<sub>2</sub>, and photoelectro-Fenton, all of which have shown promising yields, as can be seen in Table 1. However, these processes require energy (and thus a relatively high operating cost), necessitating an alternative approach to degrade pharmaceuticals such as LOS. This alternative could be the use of heterogeneous processes. For instance, Andrade et al. [43] used N-doped porous carbon to activate PMS and achieved complete LOS removal after 240 min of reaction time. However, there is no data on LOS degradation or *E. coli* inactivation using a Mo<sub>2</sub>C/SPS process.

**Table 1.** Degradation of LOS using various AOPs.

Process	Conditions	LOS Removal	Reference
Electrochemical oxidation	[LOS] <sub>0</sub> = 377 μM, [Na <sub>2</sub> SO <sub>4</sub> ] = 0.05 M, BDD anode, SS cathode, J = 80 mA/cm <sup>2</sup> , pH = 7	100% in 180 min (UPW) -	[44]
Ultrasound	[LOS] <sub>0</sub> = 40 μM, P = 88 W/L, pH = 6.5, 20 °C	100% in 120 min (UPW) 100% in 120 min (hospital wastewater)	[16]
UVC/Fe <sup>2+</sup> /H <sub>2</sub> O <sub>2</sub>	[LOS] <sub>0</sub> = 40 μM, [Fe <sup>2+</sup> ] = 40 μM, [H <sub>2</sub> O <sub>2</sub> ] = 400 μM, pH = 6.1, 23 °C	76% TOC in 120 min (UPW) 30% TOC in 120 min (groundwater)	[17]
N-doped porous carbon and PMS	[LOS] <sub>0</sub> = 40 μM, [catalyst] = 26 mg/L, [PMS] = 6.5 mM, pH = 5.2, 25 °C	100% (240 min) 96% in 240 min (20 mg/L humic acid)	[43]
UVC/H <sub>2</sub> O <sub>2</sub>	[LOS] <sub>0</sub> = 43.4 μM, [H <sub>2</sub> O <sub>2</sub> ] = 500 μM pH 6.1	65.7% in 20 min (distilled water) ≈27% in 20 min (fresh urine)	[45]
Photoelectron Fenton	[LOS] <sub>0</sub> = 45 μM, [Na <sub>2</sub> SO <sub>4</sub> ] = 0.05 M, [Fe <sup>2+</sup> ] = 36 μM, BDD anode, SS cathode, j = 5 mA/cm <sup>2</sup> , UVA = 1.4 W/m <sup>2</sup> , pH = 3	≈95% (30 min) -	[46]
Heat/US/SPS	[LOS] <sub>0</sub> = 1.18 μM, [SPS] = 200 μM, US = 36 W/L, 20 kHz, 50 °C, pH = 5.25	100% in 15 min (UPW) 60% in 45 min (WW)	[47]
Biochar from spent malt rootlet treated with acid and SPS	[LOS] <sub>0</sub> = 0.59 μM, [SPS] = 1.05 mM, [Acid-C] = 90 mg/L pH = 5.6, 25 °C	91% in 90 min (UPW) 20% in 90 min (WW)	[48]
Mo <sub>2</sub> C and SPS	[LOS] <sub>0</sub> = 1.18 μM, [SPS] = 1.05 mM, [Mo <sub>2</sub> C] = 500 mg/L pH = 5.5, 25 °C	100% in 45 min (UPW) 34% in 45 min (WW)	This study

Furthermore, a promising strategy to enhance treatment performance is the concurrent use of multiple processes. Although some studies have investigated the use of treated molybdenum carbide to activate PMS, a combination of these systems with renewable energy provided by solar irradiation is an intriguing strategy towards enhanced efficiency. At the same time, most published studies are limited to the examination of the efficiency over a probe compound, while the use of the proposed hybrid system as a tertiary treatment (i.e., including disinfection) has not been explored.

In summary, to the best of the authors' knowledge, there is no data on losartan degradation via the Mo<sub>2</sub>C/SPS process or the synergistic effect of the Mo<sub>2</sub>C/SPS process combined with solar irradiation for the simultaneous elimination of losartan and inactivation of *E. coli*. Therefore, this study aims at (i) investigating the effects of different oxidants, catalysts, SPS and LOS concentrations, initial solution pH, synthetic and real water matrices on LOS oxidation and the degradation reaction mechanism using various scavengers, as well as Mo<sub>2</sub>C reusability; (ii) testing the ability of the Mo<sub>2</sub>C/SPS process to eliminate pathogenic microorganisms; and (iii) examining the synergistic effects of a hybrid process for simultaneous losartan elimination and *E. coli* inactivation by coupling Mo<sub>2</sub>C/SPS with simulated solar irradiation.

## 2. Results and Discussion

### 2.1. Mo<sub>2</sub>C Characterization

Figure 1 shows the X-ray diffraction pattern of the Mo<sub>2</sub>C used in the present study. The typical crystal planes (100), (002), (101), (102), (110), (103), (112), and (201) of Mo<sub>2</sub>C (JCPDS No 01-1188) are clearly discernible [49–51]. In addition, its primary crystallite size, as estimated using the Debye–Scherrer formula, was found to be equal to 35 nm.

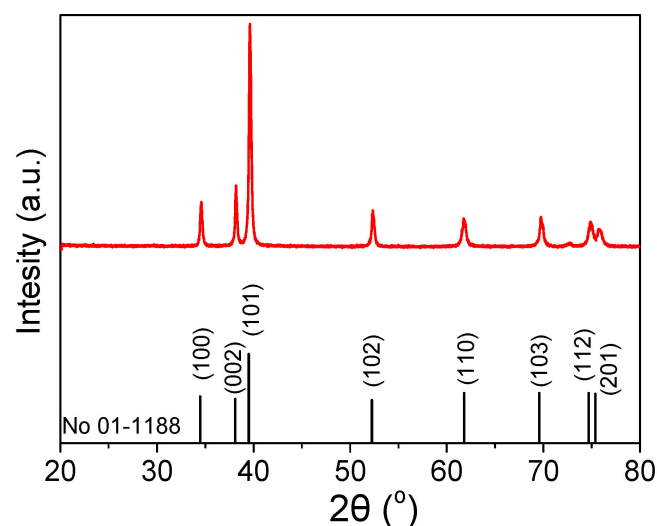
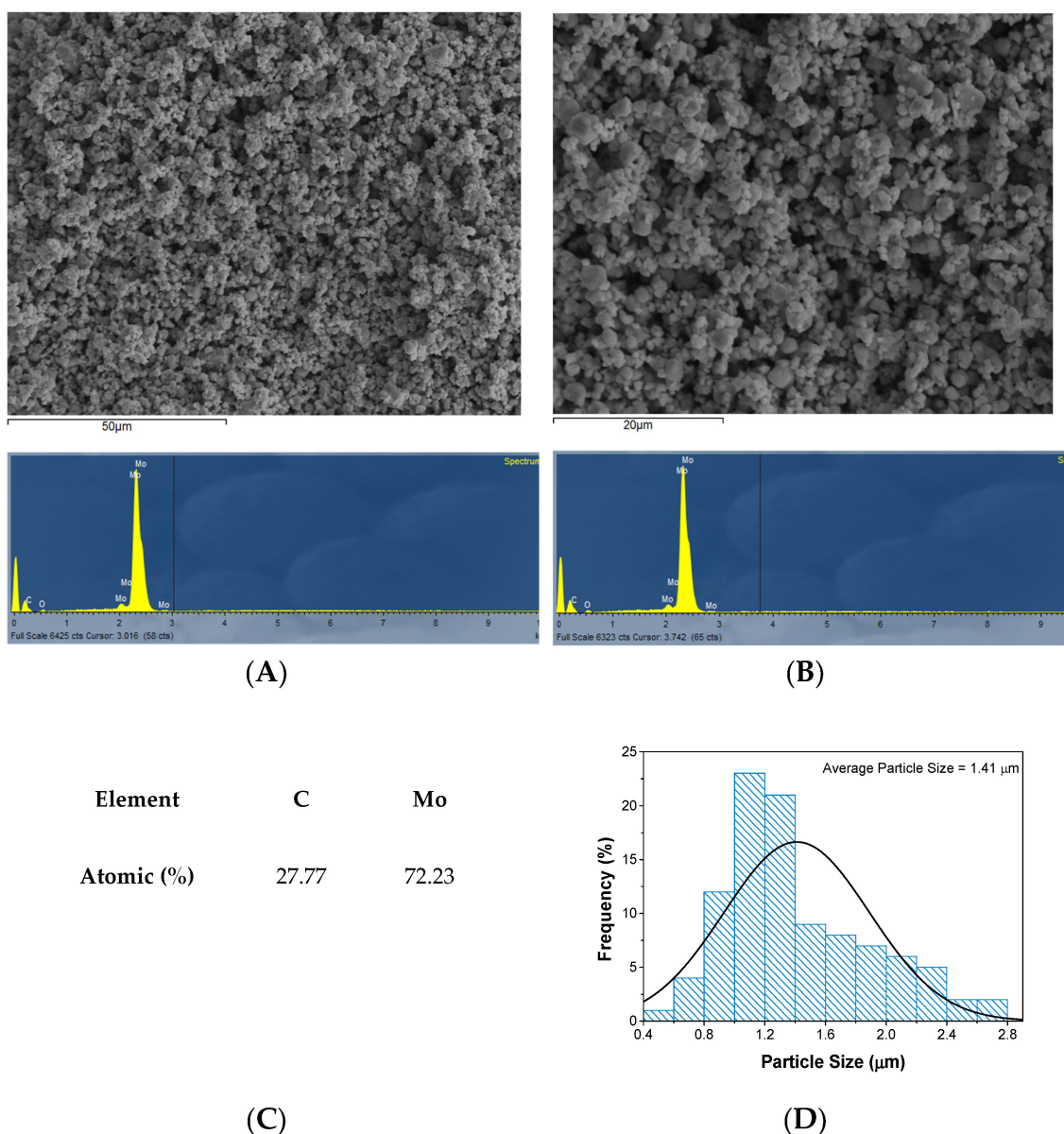


Figure 1. XRD pattern of Mo<sub>2</sub>C.

The zeta potential of Mo<sub>2</sub>C was measured in ultrapure water at various pH values to determine its isoelectric point. The calculated p*H*<sub>ZPC</sub> (pH at zero-point charge) was found to be equal to 3.7, which is consistent with previous studies [42].

The morphology of Mo<sub>2</sub>C was studied by means of SEM/EDS, and characteristic images are shown in Figure 2. It was observed that Mo<sub>2</sub>C consisted of almost spherical particles agglomerated with each other homogeneously with an estimated average diameter of approximately 1.41 μm (Figure 2D). Moreover, it could be stated that particle size distribution (Figure 2D) was rather broad, including particles from 0.4 to ca. 2.8 μm [52]. In addition, EDS spectra confirmed the presence of Mo, O and C alone without impurities.



**Figure 2.** (A,B) Characteristic SEM images of  $\text{Mo}_2\text{C}$  at different magnifications with the corresponding EDS spectra. (C) Atomic percentage of  $\text{Mo}_2\text{C}$  elements. (D) Particle size distribution of  $\text{Mo}_2\text{C}$ .

## 2.2. Catalytic Results

### 2.2.1. Activation of Various Types of Oxidants

The decomposition of 500  $\mu\text{g/L}$  LOS using 500  $\text{mg/L}$   $\text{Mo}_2\text{C}$  to activate sodium metaperiodate ( $\text{NaIO}_4$ ), sodium percarbonate ( $\text{Na}_2\text{H}_3\text{CO}_6$ ),  $\text{H}_2\text{O}_2$ , and SPS was examined, and the results are displayed in Figure 3. The concentration of oxidants used was 1.05 mM. A complete degradation of LOS was achieved using  $\text{Mo}_2\text{C}$ -SPS after 45 min of reaction, whereas in the cases of  $\text{Mo}_2\text{C}$ - $\text{NaIO}_4$ ,  $\text{Mo}_2\text{C}$ - $\text{H}_2\text{O}_2$ , and  $\text{Mo}_2\text{C}$ - $\text{Na}_2\text{H}_3\text{CO}_6$ , only 58%, 39%, and 17% of LOS removal were achieved after 45 min, respectively. These results clearly demonstrate the superiority of SPS over  $\text{NaIO}_4$ ,  $\text{H}_2\text{O}_2$  and  $\text{Na}_2\text{H}_3\text{CO}_6$  when  $\text{Mo}_2\text{C}$  is used as the activator since the decomposition rate, as demonstrated by the computed  $k_{\text{app}}$  values, is 1–2 orders of magnitude greater. Similar results were reported by Bao et al. [42] and Yang et al. [38]. Bao et al. [42] investigated the degradation of 5  $\text{mg/L}$  carbamazepine with 300  $\text{mg/L}$   $\text{Mo}_2\text{C}/\text{C}$  and 0.75 mM PMS. They found that the  $\text{Mo}_2\text{C}/\text{C}$ -PMS process could degrade carbamazepine after 75 min of reaction. Meanwhile, Yang et al. [38] studied the

degradation of 40 mg/L tetracycline with 300 mg/L 5% Cu-Mo<sub>2</sub>C and 300 mg/L PMS. They reported a complete degradation of tetracycline after 20 min of reaction.

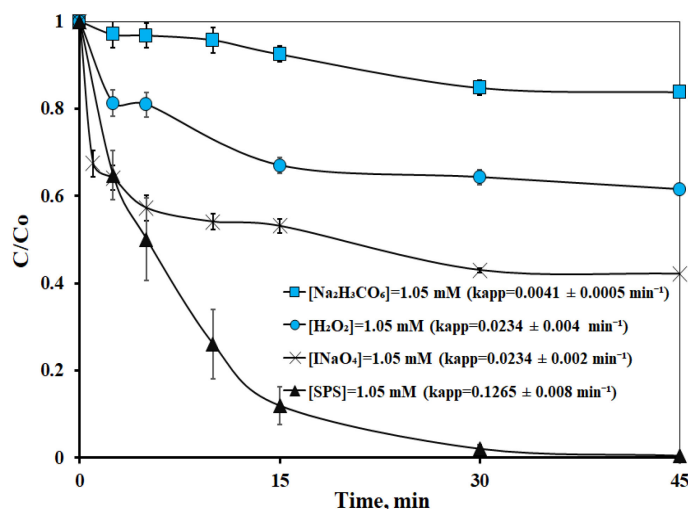


**Figure 3.** Performance of Mo<sub>2</sub>C in activating various oxidants for 500 µg/L LOS degradation in UPW and inherent pH ≈ 5.5. Experimental conditions: [Mo<sub>2</sub>C] = 500 mg/L, [NaIO<sub>4</sub>] = [Na<sub>2</sub>H<sub>3</sub>CO<sub>6</sub>] = [H<sub>2</sub>O<sub>2</sub>] = [SPS] = 1.05 mM.

Thus, both pure Mo<sub>2</sub>C and modified Mo<sub>2</sub>C-based catalysts are capable of activating SPS and PMS, respectively. However, it should be noted that none of the aforementioned studies thoroughly examined the ability of pure, unmodified Mo<sub>2</sub>C to activate SPS, which is a less expensive oxidant than PMS.

Interestingly, the Mo<sub>2</sub>C/persulfate system has the capability to generate different reactive species, including sulfate and hydroxyl radicals and singlet oxygen. More researchers are attributing this high efficiency to the redox potential of the formed radicals [53], as well as to higher electrostatic adsorption and collision efficiency. Although the activation of hydrogen peroxide can generate hydroxyl radicals with high redox potential, they are also characterized by no selectivity and a very short lifetime. Conversely, the persulfate system also produces carbonate radicals with higher selectivity but reduced redox potential [53]. Meanwhile, NaIO<sub>4</sub> has a redox potential of 1.60 V. However, oxidation reactions initiated by this ion are known to be selective and significantly slower than those involving hydroxyl and sulfate radicals [54]. Therefore, in this study, Mo<sub>2</sub>C was chosen as the activator and SPS as the oxidant for the degradation of LOS for further study.

### 2.2.2. Effect of Operating Parameters (Initial Concentration of Catalyst, Persulfate, Losartan, and pH)

It is well known that parameters such as the pH of the solution and the concentrations of catalysts, oxidants, and micropollutants can all affect catalytic performance.

Figure 4A shows that by increasing Mo<sub>2</sub>C concentration, both the degradation rate and the adsorption of 500 µg/L LOS increased. Specifically, 41%, 63%, 88%, and 93% of LOS removal were achieved with 125, 250, 500, and 750 mg/L Mo<sub>2</sub>C, respectively, after 15 min of reaction, while LOS adsorption rose from 4% for 125 mg/L Mo<sub>2</sub>C to 30% for 750 mg/L Mo<sub>2</sub>C during the same reaction time. (The respective *k<sub>app</sub>* values are shown in Figure S1.) Increasing the amount of Mo<sub>2</sub>C meant that more active sites were available for LOS adsorption and SPS activation, leading to faster degradation rates. However, as seen in Figure 4A, LOS degradation with 750 mg/L Mo<sub>2</sub>C was not significantly faster than that for 500 mg/L Mo<sub>2</sub>C; thus, the chosen catalyst concentration was 500 mg/L. Moreover, an additional experiment was carried out in the absence of Mo<sub>2</sub>C to investigate the potential of SPS to oxidize LOS as a mild oxidant; only 20% LOS removal was achieved after 45 min of reaction.

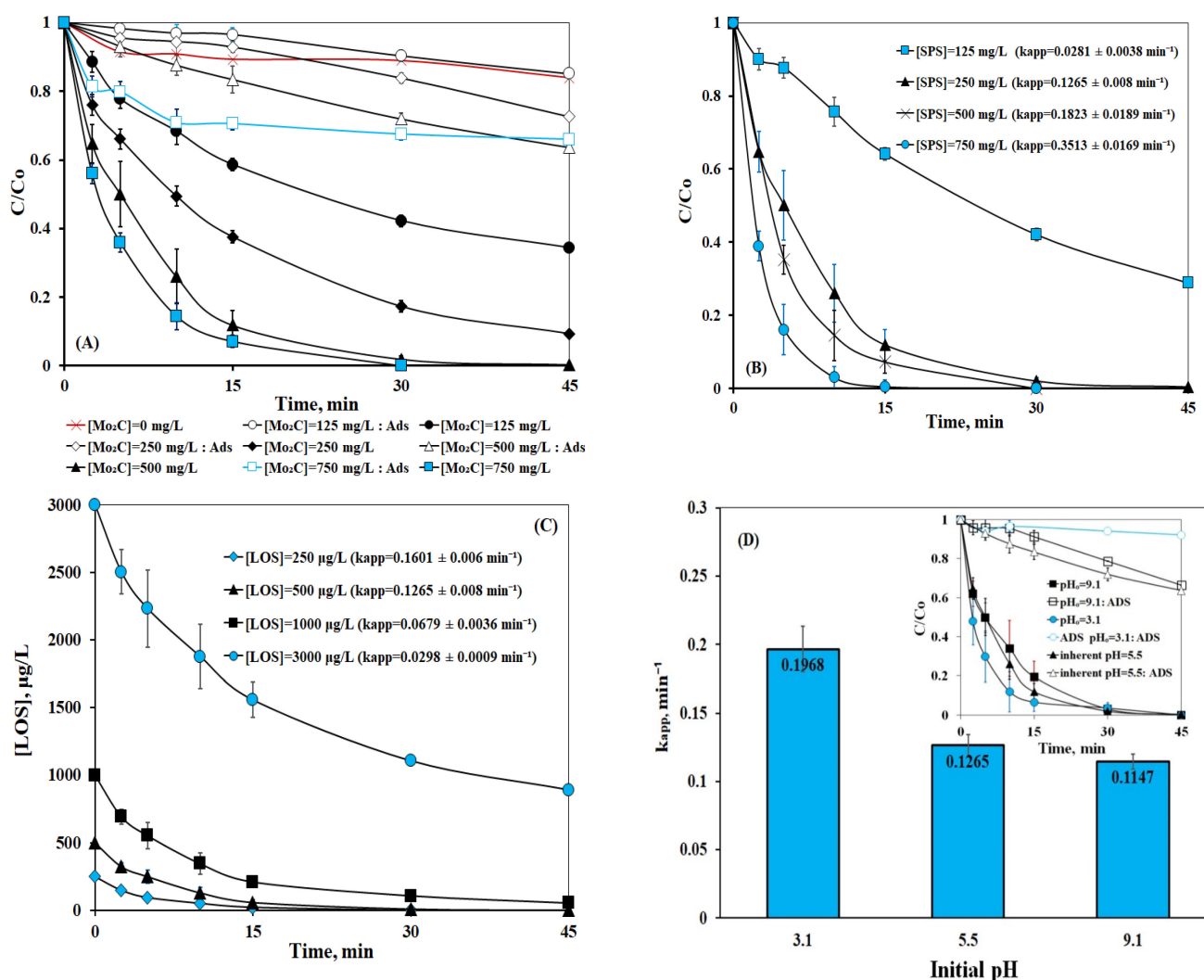


**Figure 4.** Effect of (A) initial concentration of catalyst on 500 µg/L LOS degradation with 250 mg/L SPS, (B) initial concentration of persulfate on 500 µg/L LOS degradation with 500 mg/L  $Mo_2C$ , (C) initial concentration of LOS on its degradation with 500 mg/L  $Mo_2C$  and 250 mg/L SPS, and (D) initial pH on 500 µg/L LOS degradation with 500 mg/L  $Mo_2C$  and 250 mg/L SPS in UPW.

Consequently, several SPS concentrations (125, 250, 500, 750 mg/L) were tested; the results are displayed in Figure 4B, showing that the yield increased as SPS concentration increased.  $k_{app}$  values increased 4.5-fold when SPS concentration rose from 125 to 250 mg/L. Further increases in SPS concentration led only to 1.44-fold and 2.78-fold higher  $k_{app}$  for 500 mg/L, and 750 mg/L SPS, respectively, using the  $k_{app}$  value for 250 mg/L SPS as a reference. Taking into consideration the environmental impact that the generated sulfate anions would have on aquatic systems, as well as the yield of the present process, 250 mg/L SPS was selected for further experiments [55].

Figure 4C presents concentration–time profiles for different initial LOS concentrations, as well as their respective  $k_{app}$  values. Although the rate constant decreased as the initial LOS concentration increased (i.e., over five-fold, from 250 to 3000 µg/L LOS), the  $Mo_2C$ /SPS process was capable of degrading efficiently relatively high concentrations of LOS; such concentrations are likely to occur in hospital wastewaters but not in secondary treated effluents or surface waters [56]. After 15 min of reaction, the remaining quantity of LOS was 1559, 211, 59, and 23 µg/L for 3000, 1000, 500, and 250 µg/L initial LOS concentration, respectively. It is worth noting that, despite the 48% degradation observed after 45 min of oxidation for 3000 µg/L of LOS, the TOC removal after 45 min was only 14%.

This indicates the production of transformation products, as already demonstrated in other advanced oxidation processes [47].

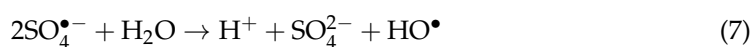
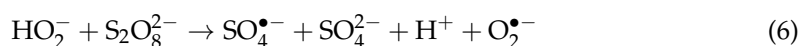
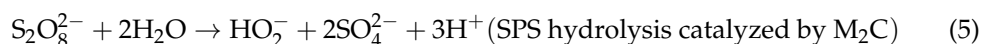
Solution pH may be an important operating parameter since real water matrices have different pH values than that of UPW, which is  $\approx 5.5$ . Therefore, adsorption and oxidation experiments were conducted at pH = 3.1 and pH = 9.1. As seen in Figure 4D, LOS degradation was favored under acidic conditions (94% LOS removal in 15 min) and slightly inhibited as the pH value increased (88% and 80% LOS removal after 15 min at pH 5.5 and 9.1, respectively). The  $k_{app}$  value decreased only 1.72 times as pH increased from 3.1 to 9.1. In contrast to oxidation, LOS adsorption was favored at an inherent pH  $\approx 5.5$ ; there was a slight reduction in LOS adsorption at pH = 9.1, while at pH = 3.1 it was almost completely inhibited. The zero-point charge of  $\text{Mo}_2\text{C}$  is 3.7, while the pKa value of LOS is 5.05 [47]. Thus, at pH = 3,  $\text{Mo}_2\text{C}$  is positively charged, and LOS exists in neutral form, while at inherent pH and pH = 9, both  $\text{Mo}_2\text{C}$  and LOS are negatively charged. As a result, the adsorption mechanism cannot be claimed to be due to repulsive/electrostatic forces but to  $\pi$ - $\pi$  interactions [57–59], which are not favored below pH = 3.

Therefore, the high degradation efficiency at pH = 3 is likely attributed to the higher adsorption of  $\text{S}_2\text{O}_8^{2-}$  on the positively charged surface of  $\text{Mo}_2\text{C}$ , resulting in the formation of more sulfate radicals.

### 2.2.3. Effect of Scavengers

Molybdenum is renowned for its various oxidation states (II, IV, VI), indicating a high electron mobility and leading to the generation of reactive species with high redox potential, such as  $\text{SO}_4^{\bullet-}$ ,  $\text{HO}^\bullet$ , and  $^1\text{O}_2$ .

To evaluate the contribution of singlet oxygen, sulfate, and hydroxyl radicals, 9.24 mM of  $\text{NaN}_3$ , MeOH, and t-BuOH were used as scavengers, respectively. As depicted in Figure 5, the introduction of each scavenger reduced process efficiency, with  $\text{NaN}_3$  resulting in the most severe inhibition, wherein the  $k_{app}$  value decreased almost 22 times. On the other hand, the  $k_{app}$  value decreased almost 2.5 and 5 times after the addition of t-BuOH and MeOH, respectively. These results suggest that all examined reactive species contribute to the oxidation of LOS via the multivalent characteristics of Mo, with singlet oxygen being the predominant reactive species. A plausible mechanism of SPS activation by  $\text{Mo}_2\text{C}$  can be described by Equations (1)–(10).





The contributions of  $\text{HO}^\bullet$ ,  $\text{SO}_4^{\bullet-}$ , and  ${}^1\text{O}_2$  were also reported by Bao et al. [42], who studied the degradation of carbamazepine using  $\text{Mo}_2\text{C}/\text{C}$  and PMS, and Yang et al. [38], who investigated the degradation of tetracycline using 5%  $\text{Cu}/\text{Mo}_2\text{C}$  and PMS. However, in their studies, sulfate radicals were reported to be the dominant reactive species, unlike in the present work.

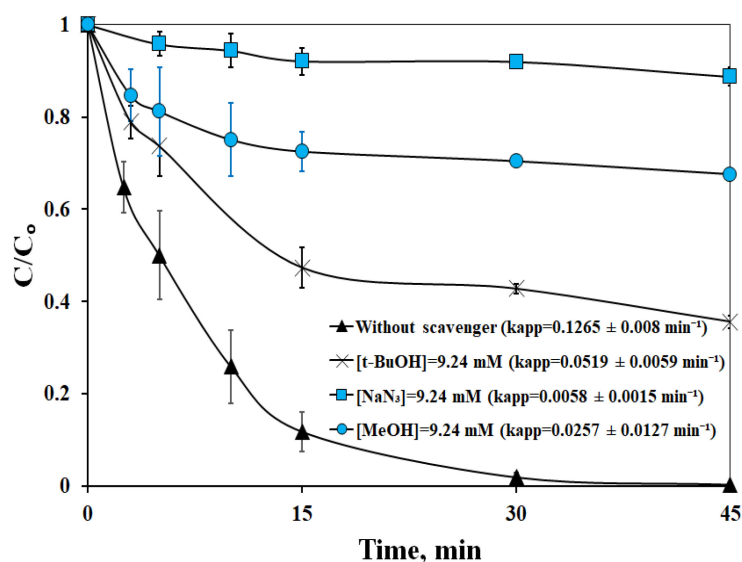
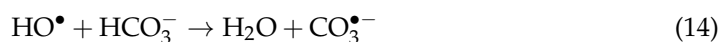
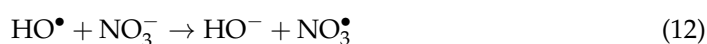
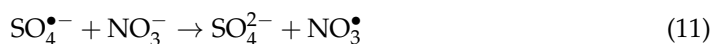


**Figure 5.** Effect of reactive species scavengers on 500 µg/L LOS degradation with 500 mg/L  $\text{Mo}_2\text{C}$  and 250 mg/L SPS in UPW.

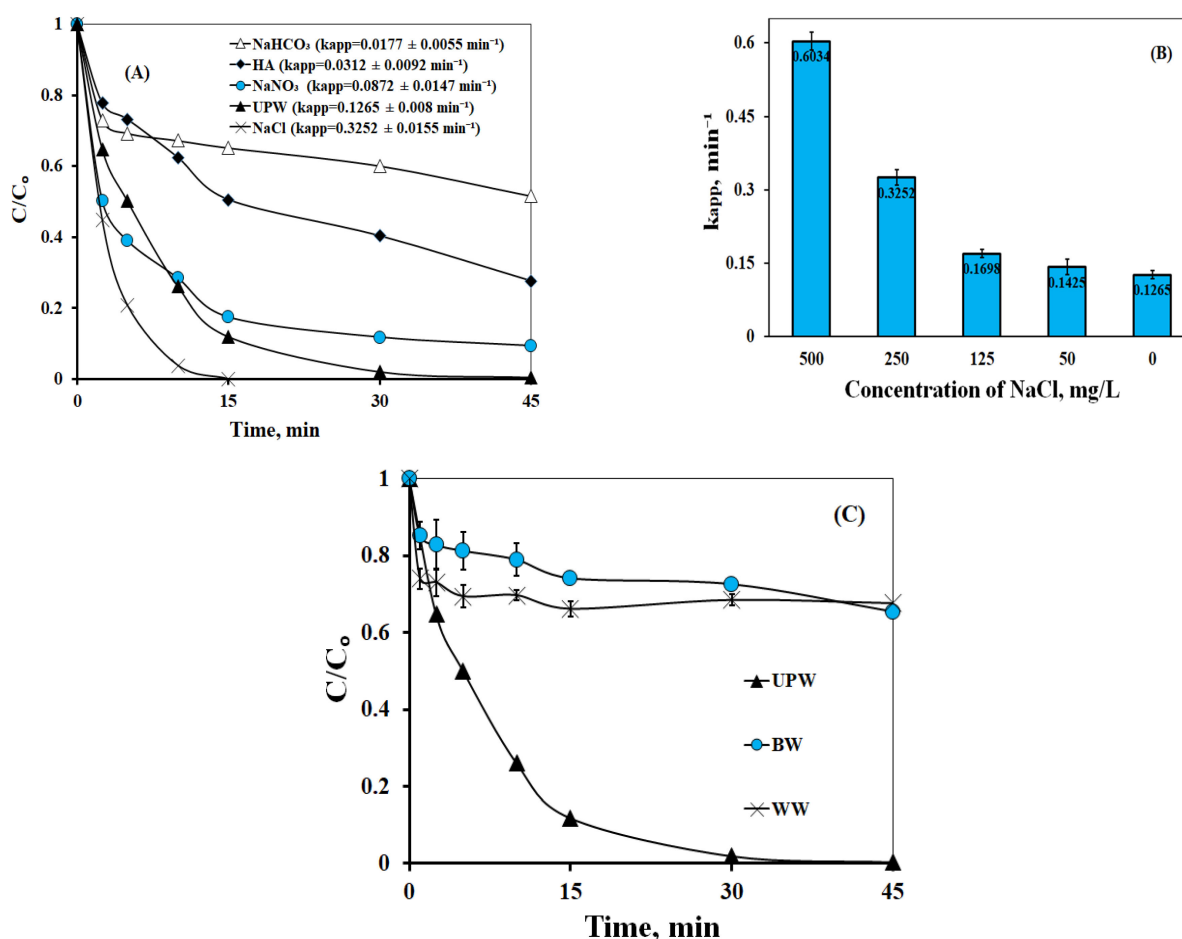
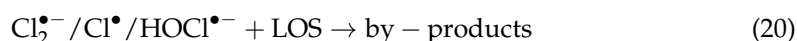
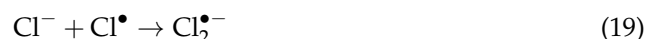
#### 2.2.4. Effect of Water Matrix

Figure 6A illustrates how LOS degradation was affected by the addition of 10 mg/L HA or 250 mg/L NaCl,  $\text{NaNO}_3$ , and  $\text{NaHCO}_3$ , respectively. Considering the findings from Section 2.2.2 (i.e., pH effect) and 2.2.3, the negative impact of  $\text{HCO}_3^-$ , HA and, to a lesser extent,  $\text{NO}_3^-$  was probably not related to pH alteration since alkaline conditions did not delay LOS degradation. Consequently, it may have been due to LOS adsorption being hindered by the presence of  $\text{NO}_3^-$ ,  $\text{HCO}_3^-$ , and HA, and the competition between LOS and inorganic and organic matter for the generated reactive species ( $\text{SO}_4^{\bullet-}$ ,  $\text{HO}^\bullet$ ,  ${}^1\text{O}_2$ ,  $\text{O}_2^{\bullet-}$ ) [60].  $\text{NO}_3^-$  as well as  $\text{HCO}_3^-$  reacted with the formed reactive species, and radicals with smaller redox potential were produced, as described by Equations (11)–(15) [38,42,44,60].



Interestingly, the addition of NaCl facilitated the degradation of LOS, leading to complete LOS removal after 150 min (Figure 6A); hence, the effect of NaCl concentration was studied further. As depicted in Figure 6B, increasing NaCl concentration from 0 to 500 mg/L led to a 5-fold degradation rate increase. Chloride anions may have reacted

with hydroxyl and sulfate radicals to form active chlorine or hypochlorous reactive species, as shown in Equations (16)–(20):



**Figure 6.** (A) Effect of 10 mg/L HA and 250 mg/L NaCl, NaHCO<sub>3</sub>, and NaNO<sub>3</sub>, respectively, on LOS degradation. (B) Effect of NaCl on LOS degradation. (C) Effect of real water matrices (BW, WW) on LOS degradation. Experimental conditions: [LOS] = 500 µg/L, [Mo<sub>2</sub>C] = 500 mg/L, and [SPS] = 250 mg/L.

These results seem contradictory when compared to other studies, which documented that the addition of Cl<sup>-</sup> had either no effect on their processes [38,60] or a detrimental effect on the yield of other systems [44,61]. However, these results align with the works of Bao et al. [42] and Chen et al. [31], who studied the degradation of carbamazepine and bisphenol A using Mo<sub>2</sub>C/C and Mo<sub>2</sub>Ga<sub>2</sub>C for PMS activation, respectively. Both studies reported an enhancement in carbamazepine and bisphenol A degradation in the presence

of  $\text{Cl}^-$  and attributed it to the direct reaction of chlorine or hypochlorous reactive species with the unsaturated bonds of micropollutants.

In addition, real water matrices were used (BW and WW) and the results are shown in Figure 6C. Only 25% and 34% of LOS removal were achieved after 15 min in BW and WW, respectively, while in UPW, more than 90% of LOS removal was achieved. This decrease in performance in real matrices was attributed to the presence of inorganic and organic matter, with  $\text{HCO}_3^-$  having the highest concentration among them (Table S1). However, it should be noted that the aim of the present work was not to optimize the system, but to study how the system was affected by various operating parameters. Therefore, the optimization of the  $\text{Mo}_2\text{C}/\text{SPS}$  system should be undertaken under representative conditions if the proposed process is to be scaled up from the lab to a pilot unit.

### 2.2.5. Reuse

Eventually, the  $\text{Mo}_2\text{C}/\text{SPS}$  system was evaluated in terms of catalyst reusability according to the following procedure: The mixture was allowed to react for 45 min. After this period, LOS conversion was measured, the mixture was centrifuged, the  $\text{Mo}_2\text{C}$  sample was collected, dried for 12 h, weighed, and then used for the degradation of another LOS solution and repetition of the experiment. This cycle was run five times (including the fresh sample) and, in all cases, a complete LOS conversion was achieved, indicating a high stability of  $\text{Mo}_2\text{C}$ , as seen in Figure S3. Moreover, the stability of the reused  $\text{Mo}_2\text{C}$  was corroborated by XRD analysis, as shown in Figure S2. It was observed that  $\text{Mo}_2\text{C}$  remained practically intact after exposure to reaction conditions for 225 min, with the primary crystallite size remaining unchanged and equal to 35 nm.

### 2.3. Disinfection and Synergistic Effects with Simulated Solar Irradiation

In a final set of experiments, the  $\text{Mo}_2\text{C}/\text{SPS}$  process was assessed as a disinfectant agent. Adsorption, blank, and degradation experiments were performed in the presence of 500  $\mu\text{g}/\text{L}$  LOS and  $\approx 10^6$ – $10^7$  CFU/mL *E. coli*. Figure 7A illustrates the degradation of LOS, while Figure 7B shows the reduction in *E. coli* population. The presence of *E. coli* significantly impacted the degradation and adsorption of LOS. Only 17% LOS removal and 10% LOS adsorption were observed after 60 min, while the *E. coli* population declined by  $1.23 \pm 0.11$  log and  $0.9 \pm 0.12$  log at the same time during the oxidation and adsorption experiment, respectively. After 60 min, no further *E. coli* inactivation and adsorption were observed, whereas in the case of LOS, slow oxidation was noted, with 30% LOS removal after 180 min of reaction. These results suggest that both LOS and *E. coli* competed for the active centers on the  $\text{Mo}_2\text{C}$  surface and for the generated reactive species.

To accelerate the degradation of LOS and *E. coli*, a coupling of the  $\text{Mo}_2\text{C}/\text{SPS}$  process with simulated solar irradiation was conducted. The choice of simulated solar radiation was made on the basis that in real-world conditions, solar irradiation is a cost-free, green energy source that is abundant on Earth.

As observed in Figure 7, the solar/SPS process exhibited a high efficiency for LOS degradation, while as for *E. coli* inactivation, the yield of the solar/SPS process was relatively poor. After 180 min of reaction, 95% LOS oxidation and  $1.30 \pm 0.13$  log *E. coli* elimination were achieved. Regarding the inactivation of *E. coli* by the solar/SPS process, similar results were reported by Wang et al. [62], who studied *E. coli* inactivation by visible light persulfate activation. Specifically, they mentioned that a system using visible light with 1 mM persulfate was not able to reduce the population of *E. coli*. However, when the persulfate concentration increased to 4 mM, they reported a 7 log *E. coli* elimination after 80 min [62].

The way reactive species inactivate/eliminate *E. coli* is similar to the mechanism proposed by Wang et al. [62] and Wang et al. [63], who studied the hybrid processes of heat/visible light/persulfate and visible light/hydrochar/persulfate for *E. coli* inactivation, respectively. They reported that reactive species cause severe damage to the cell membrane. The reactive species then pass through the membrane, and the cell's defense system tries

to protect itself by producing a high level of intracellular antioxidant enzymes. But as the reactive species continually penetrate through the membrane, the defense systems become incapacitated, leading to the destruction of the cell.

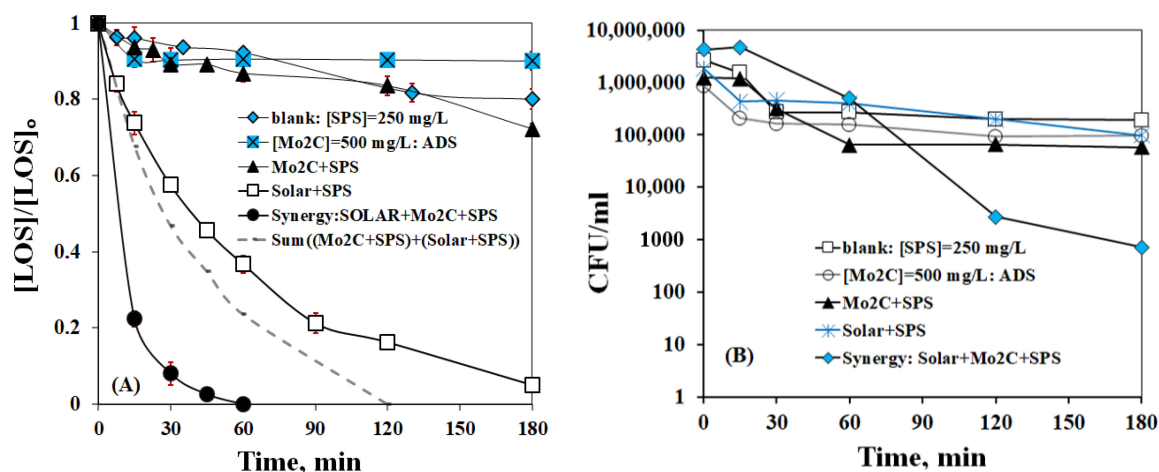


**Figure 7.** Simultaneous degradation of 500 µg/L LOS (A) and inactivation of  $\approx 10^6$ – $10^7$  CFU/mL *E. coli* (B) in UPW with 500 mg/L Mo<sub>2</sub>C and 250 mg/L SPS and the synergistic effects with simulated solar irradiation.

However, the results of the synergistic solar/Mo<sub>2</sub>C/SPS process were promising for both pollutant and microorganism elimination. Complete LOS removal was achieved in 60 min, comparable to LOS degradation (100% removal in 45 min) in the absence of *E. coli*. Regarding *E. coli* inactivation performance, a reduction by  $3.98 \log \pm 0.21$  was observed, which is significantly higher than that achieved by the Mo<sub>2</sub>C/SPS and solar/SPS processes alone.

The hybrid system with  $k_{(\text{Solar}/\text{Mo}_2\text{C}/\text{SPS})} = 0.083 \pm 0.005 \text{ min}^{-1}$  exhibited a higher yield than the sum of the individual processes with  $k_{(\text{Mo}_2\text{C}/\text{SPS})} = 0.0024 \pm 0.003 \text{ min}^{-1}$  and  $k_{(\text{solar}/\text{SPS})} = 0.0165 \pm 0.004 \text{ min}^{-1}$ , as seen in Figure 7A (curve with dotted lines). The extent of synergy, *S*, for LOS decomposition may be computed as follows:

$$S = \frac{k_{\text{Solar}/\text{Mo}_2\text{C}/\text{SPS}}}{k_{\text{Mo}_2\text{C}/\text{SPS}} + k_{\text{solar}/\text{SPS}}} \quad \text{where, } S = \begin{cases} S > 1 (\text{synergistic effect}) \\ S = 1 (\text{additive effect}) \\ S < 1 (\text{antagonistic effect}) \end{cases} \quad (21)$$

Subsequently, the value of *S* from the data in Figure 7A is 4.4.

To examine the observed synergy, an additional experiment was conducted for the simultaneous removal of LOS and *E. coli* using the Mo<sub>2</sub>C/solar system in the absence of the oxidant. Despite the fact that, according to the literature, the energy gap of Mo<sub>2</sub>C is 1.22 V [64], the obtained results were similar to adsorption (i.e., absence of light and oxidant). A possible explanation may be the position of the conduction and valence bands of Mo<sub>2</sub>C, which are −0.41 V and 0.81 V, respectively [64]. Therefore, the photogenerated holes have very low oxidation potential, while the Mo<sub>2</sub>C/solar system is incapable of producing hydroxyl radicals. On the other hand, SPS can trap the photogenerated electrons, thus increasing the separation of photoproduced holes and electrons and producing additional reactive species into the system through oxidant activation by the photoproduced electrons. Therefore, the observed synergy can be justified by the higher concentration of reactive species and the different activation mechanisms in the combined system. Thus, the role of solar irradiation is associated with an acceleration of the production of additional SO<sub>4</sub><sup>•−</sup> and HO<sup>•</sup> through SPS activation, which consequently leads to the formation of more O<sub>2</sub><sup>•−</sup> and <sup>1</sup>O<sub>2</sub> (Equations (6), (8), and (9)), which are available for the degradation of LOS and *E. coli*. In summary, in the hybrid system, persulfate is activated in three ways: (i) homogeneously by solar irradiation, which allows a direct attack on LOS molecules and

on the cell membranes of *E. coli*, (ii) heterogeneously by Mo<sub>2</sub>C, and (iii) photocatalytically by the photogenerated electrons.

### 3. Materials and Methods

#### 3.1. Materials

Molybdenum carbide (Mo<sub>2</sub>C ≥ 99.5%, CAS: 12069-89-5), sodium (meta)periodate (NaIO<sub>4</sub> ≥ 99.0%, CAS: 7790-28-5), sodium nitrate (NaNO<sub>3</sub> ≥ 99.0%, CAS: 7631-99-4), sodium persulfate (SPS ≥ 99.5%), losartan potassium (LOS), humic acid (HA, technical grade), Petri dishes (D = 9 cm), tert-butyl alcohol (t-BuOH), sodium azide (NaN<sub>3</sub>), sodium bicarbonate (NaHCO<sub>3</sub>), ortho-phosphoric acid (H<sub>3</sub>PO<sub>4</sub> ≥ 85%), and sulfuric acid (H<sub>2</sub>SO<sub>4</sub>) were obtained from Sigma Aldrich (St. Louis, MO, USA). Further details for the above reagents and LOS can be found in the study of Ioannidi et al. (2022). Sodium percarbonate (Na<sub>2</sub>CO<sub>3</sub>·1.5H<sub>2</sub>O<sub>2</sub>, CAS: 15630-89-4), and hydrogen peroxide solution 30% (H<sub>2</sub>O<sub>2</sub>, CAS: 7722-84-1) were bought from Acros organics (Geel, ANTWERP, Belgium) and Carlo Ebra reagents (Denzlinger Str., Emmendingen, Germany), respectively, while sodium hydroxide (NaOH, CAS: 1310-73-2), and sodium chloride (NaCl ≥ 99.5%, CAS: 16610-31000) were purchased from Penta (Radiová, Prague, Czechia). Methanol (MeOH, hplc-grade, CAS: 67-56-1) was purchased from Fischer chemicals (Riesbachstrasse, Zürich, Switzerland). All chemicals were used without any further purification. Furthermore, microbiological yeast extract (CAS:1702.00) and tryptone (CAS:1612.00) were purchased from Condalab (C. Forja, Torrejón de Ardoz, Madrid, Spain), while agar (CAS: 9002-18-0) was purchased from Serva (Carl-benz-str., Heidelberg, Baden-Wuerttemberg, Germany). *E. coli* (DSM 1103) was obtained by the Leibniz Institute DSMZ (German Collection of Microorganisms and Cell Cultures).

Most experiments were performed in ultrapure water (UPW, 18.2 MΩ·cm and pH ≈ 5.5), while commercial bottled water (BW) and secondary effluent from the University of Patras campus wastewater treatment plant (WW) were also used. Details of the water matrices can be found in Table S1.

#### 3.2. Procedure of Degradation Experiments

For LOS oxidation experiments, a batch reactor with a maximum volume capacity of 150 mL was used. The working volume of the reactor with the desired LOS concentration was 100 mL. The reaction started after the simultaneous addition of the preferred amount of Mo<sub>2</sub>C and SPS under continuous magnetic stirring. At fixed time intervals, samples of 1.2 mL were collected, quenched with 0.3 mL MeOH, and filtered through 0.22 μm PVDF filter.

To study the role of pH, 1 M NaOH and 1 M H<sub>2</sub>SO<sub>4</sub> were used. pH adjustment to 9 or 3 was performed prior to the addition of the catalyst and oxidant. During the reaction, solution pH was monitored but left uncontrolled. To investigate the contribution of several kinds of reactive species, MeOH, t-BuOH, and NaN<sub>3</sub> were used as scavengers.

#### 3.3. Experimental Procedure of Disinfection

To evaluate the potential of the Mo<sub>2</sub>C/SPS system for disinfection, *E. coli* was used as a representative Gram-negative bacterium. All experiments were conducted in the presence of 500 μg/L LOS to investigate the simultaneous degradation of xenobiotics and pathogens typically existing in secondary effluent. The necessary equipment (e.g., glass vessels, Eppendorf tubes, pipette tips, stirring magnets, beakers, nutrient medium, ultrapure water, and 0.8% w/v NaCl aqueous solution) for carrying out all inactivation experiments was sterilized in an autoclave. Details of bacteria cultivation, concentration estimation, and the execution of inactivation experiments can be found in the supplementary material [65–67].

#### 3.4. Analytical Methods

The concentration of LOS was monitored using a high-performance liquid chromatograph (HPLC, waters alliance 2695). Details of the analytical method can be obtained in the

study of Ioannidi et al. [47]. Total organic carbon (TOC) was measured using a Shimadzu TOC-L<sub>CSH</sub> analyzer (Kyoto, Japan).

### 3.5. Mo<sub>2</sub>C Characterization

Scanning electron microscopy (JEOL 6300) (Tokyo, Japan) equipped with an energy-dispersive spectrometer (EDS) was adopted to study the surface morphology and chemical composition of Mo<sub>2</sub>C, while the crystal structure of the sample was obtained by X-ray diffraction (XRD) (Bruker D8-Advanced diffractometer) (Billerica, MA, USA). Its primary crystallite size was calculated by means of the Debye–Scherrer equation [68]. A zeta potential analyzer (Zetasizer Nano Z (Malvern), UK) was employed to assess the electrical characteristics of the catalyst's solid-liquid interface within the reaction solution. Additional information can be found in former publications from our group [69].

### 3.6. Data Analysis

LOS degradation obeys a pseudo-first-order kinetic rate with  $R^2 > 0.98$  in all cases. The apparent rate constants ( $k_{app}$ , min<sup>-1</sup>) were calculated according to Equation (22):

$$\text{rate} = -\frac{d[\text{LOS}]}{dt} = k_{app}[\text{LOS}] \rightarrow \ln\left(\frac{[\text{LOS}]}{[\text{LOS}]_0}\right) = -k_{app}t \quad (22)$$

where  $[\text{LOS}]_0$ , and  $[\text{LOS}]$  refer to LOS concentration at times zero and  $t$ , respectively.

## 4. Conclusions

In this work, Mo<sub>2</sub>C, a 2D material, demonstrated notable efficiency in persulfate activation and LOS decomposition. The primary conclusions of this work can be summarized as follows:

- The investigated system was capable of eliminating 500 µg/L of LOS in less than 45 min. This concentration is well over the upper limit typically found in surface waters and/or secondary treated effluents, which implies that milder treatment conditions would suffice to deal with environmentally relevant concentrations.
- Oxidation adhered to pseudo-first-order kinetics, and the apparent kinetic constant decreased with increasing LOS concentration and increased in acidic pH.
- The presence of organic matter and carbonate impeded LOS degradation in the experiments conducted in secondary effluent and bottled water; moreover, the presence of *E. coli* slowed down LOS decomposition, while *E. coli* removal was only 1.23 log after 180 min. This clearly highlights the critical role of the environmentally relevant water matrix.
- Sulfate radicals, hydroxyl radicals, and singlet oxygen participated in LOS destruction, but singlet oxygen emerged as the predominant species. In this respect, the possible interplay between catalyst, oxidants, and the target and non-target species may be quite complicated.
- Experiments conducted in the presence of simulated solar irradiation demonstrated a significant synergy and efficiency improvement, leading to complete LOS elimination in 60 min and nearly a 4-log reduction of *E. coli* in 180 min. This implies that process coupling may be a step in the right direction in terms of enhancing treatment efficiency; nonetheless, this should be complemented by cost-efficient strategies that can be offered by the application of renewable energy sources.
- Though the use of 2D materials in environmental remediation appears as a promising strategy, further research is needed to examine the operation of similar systems under continuous flow, and scaling up is required. Future work must also delve deeper into the mechanism and transformation products, as well as investigate toxicity and Mo leaching during the treatment.

**Supplementary Materials:** The following supporting information can be downloaded at: <https://www.mdpi.com/article/10.3390/catal13091285/s1>, Figure S1: Apparent rate constants at several initial concentrations of Mo<sub>2</sub>C for LOS degradation and adsorption in UPW. Experimental conditions: [LOS] = 500 µg/L, and [SPS] = 250 mg/L; Figure S2: XRD patterns of the “fresh” Mo<sub>2</sub>C, and after exposure to reaction conditions for 225 min (500 mg/L Mo<sub>2</sub>C, 250 mg/L SPS and 500 µg/L LOS); Figure S3. Reuse experiments of Mo<sub>2</sub>C for LOS removal in UPW. Experimental conditions: [Mo<sub>2</sub>C] = 500 mg/L, [SPS] = 250 mg/L, and [LOS] = 500 µg/L at inherent pH ≈ 5.5.; Table S1: Main properties of various water matrices used in this study.

**Author Contributions:** Conceptualization, A.A.I.; Z.F. and D.M.; methodology, A.A.I., A.P., E.K., M.K. and D.M.; formal analysis, A.A.I., M.V., Z.F. and A.P.; investigation, A.A.I., M.V., E.K. and A.P.; resources, Z.F., M.K. and D.M.; data curation, A.A.I., M.V. and A.P.; writing—original draft preparation, A.A.I., Z.F. and A.P.; writing—review and editing, A.A.I., A.P., E.K., M.K. and D.M.; visualization, A.A.I., M.V. and A.P.; supervision, D.M.; funding acquisition, D.M. All authors have read and agreed to the published version of the manuscript.

**Funding:** Alexandra Ioannidi acknowledges that the implementation of the doctoral thesis was co-financed by Greece and the European Union (European Social Fund-ESF) through the Operational Programme “Human Resources Development, Education and Lifelong Learning” in the context of the Act “Enhancing Human Resources Research Potential by undertaking a Doctoral Research” Sub-action 2: IKY Scholarship Program for PhD candidates in the Greek Universities.

**Data Availability Statement:** Not applicable.

**Conflicts of Interest:** The authors declare no conflict of interest.

## References

1. Ekramul Mahmud, H.N.M.; Huq, A.K.O.; Yahya, R.B. The removal of heavy metal ions from wastewater/aqueous solution using polypyrrole-based adsorbents: A review. *RSC Adv.* **2016**, *6*, 14778–14791. [CrossRef]
2. Priya, A.K.; Gnanasekaran, L.; Rajendran, S.; Qin, J.; Vasseghian, Y. Occurrences and removal of pharmaceutical and personal care products from aquatic systems using advanced treatment- A review. *Environ. Res.* **2022**, *204*, 112298. [CrossRef]
3. Asghar, M.A.; Zhu, Q.; Sun, S.; Peng, Y.; Shuai, Q. Suspect screening and target quantification of human pharmaceutical residues in the surface water of Wuhan, China, using UHPLC-Q-Orbitrap HRMS. *Sci. Total Environ.* **2018**, *635*, 828–837. [CrossRef]
4. Busch, W.; Schmidt, S.; Kühne, R.; Schulze, T.; Krauss, M.; Altenburger, R. Micropollutants in European rivers: A mode of action survey to support the development of effect-based tools for water monitoring: Micropollutants in European rivers: A mode-of-action. *Environ. Toxicol. Chem.* **2016**, *35*, 1887–1899. [CrossRef] [PubMed]
5. Kane, S.P. Valsartan, ClinCalc DrugStats Database, Version 2022.08. ClinCalc. Available online: <https://clincalc.com/DrugStats/Drugs/Valsartan> (accessed on 29 July 2023).
6. Statista: Number of Losartan Potassium Prescriptions in the U.S. from 2004 to 2020 (in Million). Available online: <https://www.statista.com/statistics/781681/losartan-potassium-prescriptions-number-in-the-us/> (accessed on 29 July 2023).
7. Centers for Disease Control and Prevention. Hypertension Cascade: Hypertension Prevalence, Treatment and Control Estimates Among U.S. Adults Aged 18 Years and Older Applying the Criteria from the American College of Cardiology and American Heart Association’s 2017 Hypertension Guideline—NHANES 2017–2020. Atlanta, GA: 12 May 2023. Available online: <https://www.cdc.gov/bloodpressure/facts.htm#:~:text=This%20includes%2037%20million%20U.S.%20adults.&text=About%2034%20million%20adults%20who,140%2F90%20mmHg%20or%20higher> (accessed on 6 July 2023).
8. Rouette, J.; McDonald, E.G.; Schuster, T.; Brophy, J.M.; Azoulay, L. Treatment and prescribing trends of antihypertensive drugs in 2.7 million UK primary care patients over 31 years: A population-based cohort study. *BMJ Open* **2022**, *12*, e057510. [CrossRef] [PubMed]
9. Cortez, F.S.; Souza, L.S.; Guimarães, L.L.; Almeida, J.E.; Pusceddu, F.H.; Maranhão, L.A.; Mota, L.G.; Nobre, C.R.; Moreno, B.B.; Abessa, D.M.S.; et al. Ecotoxicological effects of losartan on the brown mussel *Perna perna* and its occurrence in seawater from Santos Bay (Brazil). *Sci. Total Environ.* **2018**, *637–638*, 1363–1371. [CrossRef]
10. Mandaric, L.; Diamantini, E.; Stella, E.; Cano-Paoli, K.; Valle-Sistac, J.; Molins-Delgado, D.; Bellin, A.; Chiogna, G.; Majone, B.; Diaz-Cruz, M.S.; et al. Contamination sources and distribution patterns of pharmaceuticals and personal care products in Alpine rivers strongly affected by tourism. *Sci. Total Environ.* **2017**, *590–591*, 484–494. [CrossRef]
11. Nuel, M.; Laurent, J.; Bois, P.; Heintz, D.; Wanko, A. Seasonal and ageing effect on the behaviour of 86 drugs in a full-scale surface treatment wetland: Removal efficiencies and distribution in plants and sediments. *Sci. Total Environ.* **2018**, *615*, 1099–1109. [CrossRef]
12. Ashfaq, M.; Li, Y.; Wang, Y.; Chen, W.; Wang, H.; Chen, X.; Wu, W.; Huang, Z.; Yu, C.-P.; Sun, Q. Occurrence, fate, and mass balance of different classes of pharmaceuticals and personal care products in an anaerobic-anoxic-oxic wastewater treatment plant in Xiamen, China. *Water Res.* **2017**, *123*, 655–667. [CrossRef]

13. Botero-Coy, A.M.; Martínez-Pachon, D.; Boix, C.; Rincon, R.J.; Castillo, N.; Arias- Marín, L.P.; Manrique-Losada, L.; Torres-Palma, R.; Moncayo-Lasso, A.; Hernandez, F. An investigation into the occurrence and removal of pharmaceuticals in Colombian wastewater. *Sci. Total Environ.* **2018**, *642*, 842–853. [[CrossRef](#)]
14. Castro, G.; Rodríguez, I.; Ramil, M.; Cela, R. Selective determination of sartan drugs in environmental water samples by mixed-mode solid-phase extraction and liquid chromatography tandem mass spectrometry. *Chemosphere* **2019**, *224*, 562–571. [[CrossRef](#)] [[PubMed](#)]
15. Wang, J.; Wang, S. Activation of persulfate (PS) and peroxymonosulfate (PMS) and application for the degradation of emerging contaminants. *Chem. Eng. J.* **2018**, *334*, 1502–1517. [[CrossRef](#)]
16. Serna-Galvis, E.A.; Isaza-Pineda, L.; Moncayo-Lasso, A.; Hernández, F.; Ibáñez, M.; Torres-Palma, R.A. Comparative degradation of two highly consumed antihypertensives in water by sonochemical process. Determination of the reaction zone, primary degradation products and theoretical calculations on the oxidative process. *Ultrason. Sonochem.* **2019**, *58*, 104635. [[CrossRef](#)] [[PubMed](#)]
17. Kaur, B.; Dulova, N. UV-assisted chemical oxidation of antihypertensive losartan in water. *J. Environ. Manag.* **2020**, *261*, 110170. [[CrossRef](#)]
18. Matsoukas, J.; Apostolopoulos, V.; Zulli, A.; Moore, G.; Kelaidonis, K.; Moschovou, K.; Mavromoustakos, T. From Angiotensin II to Cyclic Peptides and Angiotensin Receptor Blockers (ARBs): Perspectives of ARBs in COVID-19 Therapy. *Molecules* **2021**, *26*, 618. [[CrossRef](#)]
19. Gurke, R.; Rößler, M.; Marx, C.; Diamond, S.; Schubert, S.; Oertel, R.; Fauler, J. Occurrence and removal of frequently prescribed pharmaceuticals and corresponding metabolites in wastewater of a sewage treatment plant. *Sci. Total Environ.* **2015**, *532*, 762–770. [[CrossRef](#)]
20. Ladhari, A.; La Mura, G.; Di Marino, C.; Di Fabio, G.; Zarrelli, A. Sartans: What they are for, how they degrade, where they are found and how they transform. *Sustain. Chem. Pharm.* **2021**, *20*, 100409. [[CrossRef](#)]
21. Osorio, V.; Larrañaga, A.; Aceña, J.; P'erez, S.; Barcel'ó, D. Concentration and risk of pharmaceuticals in freshwater systems are related to the population density and the livestock units in Iberian Rivers. *Sci. Total Environ.* **2016**, *540*, 267–277. [[CrossRef](#)]
22. Adams, E.; Neves, B.B.; Prola, L.D.T.; De Liz, M.V.; Martins, L.R.R.; Ramsdorf, W.A.; De Freitas, A.M. Ecotoxicity and genotoxicity assessment of losartan after UV/H<sub>2</sub>O<sub>2</sub> and UVC/photolysis treatments. *Environ. Sci. Pollut. Res.* **2021**, *28*, 23812–23821. [[CrossRef](#)]
23. Czekalski, N.; Imminger, S.; Salhi, E.; Veljkovic, M.; Kleffel, K.; Drissner, D.; Hammes, F.; Bürgmann, H.; Von Gunten, U. Inactivation of Antibiotic Resistant Bacteria and Resistance Genes by Ozone: From Laboratory Experiments to Full-Scale Wastewater Treatment. *Environ. Sci. Technol.* **2016**, *50*, 11862–11871. [[CrossRef](#)]
24. Iakovides, I.C.; Michael-Kordatou, I.; Moreira, N.F.F.; Ribeiro, A.R.; Fernandes, T.; Pereira, M.F.R.; Nunes, O.C.; Manaia, C.M.; Silva, A.M.T.; Fatta-Kassinos, D. Continuous ozonation of urban wastewater: Removal of antibiotics, antibiotic-resistant *Escherichia coli* and antibiotic resistance genes and phytotoxicity. *Water Res.* **2019**, *159*, 333–347. [[CrossRef](#)] [[PubMed](#)]
25. Nnadozie, C.F.; Odume, O.N. Freshwater environments as reservoirs of antibiotic resistant bacteria and their role in the dissemination of antibiotic resistance genes. *Environ. Pollut.* **2019**, *254*, 113067. [[CrossRef](#)] [[PubMed](#)]
26. Yoon, S.-H.; Ha, S.-M.; Kwon, S.; Lim, J.; Kim, Y.; Seo, H.; Chun, J. Introducing EzBioCloud: A taxonomically united database of 16S rRNA gene sequences and whole-genome assemblies. *Int. J. Syst. Evol. Microbiol.* **2017**, *67*, 1613–1617. [[CrossRef](#)] [[PubMed](#)]
27. Kokkinos, P.; Venieri, D.; Mantzavinos, D. Advanced Oxidation Processes for Water and Wastewater Viral Disinfection. A Systematic Review. *Food Environ. Virol.* **2021**, *13*, 283–302. [[CrossRef](#)] [[PubMed](#)]
28. García-Espinoza, J.D.; Robles, I.; Durán-Moreno, A.; Godínez, L.A. Photo-assisted electrochemical advanced oxidation processes for the disinfection of aqueous solutions: A review. *Chemosphere* **2021**, *274*, 129957. [[CrossRef](#)]
29. Chen, Y.; Duan, X.; Zhou, X.; Wang, R.; Wang, S.; Ren, N.; Ho, S.-H. Advanced oxidation processes for water disinfection: Features, mechanisms and prospects. *J. Chem. Eng.* **2021**, *409*, 128207. [[CrossRef](#)]
30. Ma, D.; Yi, H.; Lai, C.; Liu, X.; Huo, X.; An, Z.; Li, L.; Fu, Y.; Li, B.; Zhang, M.; et al. Critical review of advanced oxidation processes in organic wastewater treatment. *Chemosphere* **2021**, *275*, 130104. [[CrossRef](#)]
31. Chen, X.; Gudda, F.O.; Hu, X.; Waigi, M.G.; Gao, Y. Degradation of bisphenol A in an oxidation system constructed from Mo<sub>2</sub>C MXene and peroxymonosulfate. *npj Clean Water* **2022**, *5*, 66. [[CrossRef](#)]
32. Guo, S.; Wang, H.; Yang, W.; Fida, H.; You, L.; Zhou, K. Scalable synthesis of Ca-doped  $\alpha$ -Fe<sub>2</sub>O<sub>3</sub> with abundant oxygen vacancies for enhanced degradation of organic pollutants through peroxymonosulfate activation. *Appl. Catal. B* **2020**, *262*, 118250. [[CrossRef](#)]
33. Ghanbari, F.; Moradi, M. Application of peroxymonosulfate and its activation methods for degradation of environmental organic pollutants: Review. *Chem. Eng. J.* **2017**, *310*, 41–62. [[CrossRef](#)]
34. Forouzesh, M.; Ebadi, A.; Aghaeinejad-Meybodi, A. Degradation of metronidazole antibiotic in aqueous medium using activated carbon as a persulfate activator. *Sep. Purif. Technol.* **2019**, *210*, 145–151. [[CrossRef](#)]
35. Bekris, L.; Frontistis, Z.; Trakakis, G.; Sygellou, L.; Galiotis, C.; Mantzavinos, D. Graphene: A new activator of sodium persulfate for the advanced oxidation of parabens in water. *Water Res.* **2017**, *126*, 111–121. [[CrossRef](#)] [[PubMed](#)]
36. Zhou, H.; Lai, L.; Wan, Y.; He, Y.; Yao, G.; Lai, B. Molybdenum disulfide (MoS<sub>2</sub>): A versatile activator of both peroxymonosulfate and persulfate for the degradation of carbamazepine. *Chem. Eng. J.* **2020**, *384*, 123264. [[CrossRef](#)]

37. Alaba, P.A.; Abbas, A.; Huang, J.; Daud, W.M.A.W. Molybdenum carbide nanoparticle: Understanding the surface properties and reaction mechanism for energy production towards a sustainable future. *Renew. Sust. Energ. Rev.* **2018**, *91*, 287–300. [[CrossRef](#)]
38. Yang, L.; Chen, H.; Jia, F.; Peng, W.; Tian, X.; Xia, L.; Wu, X.; Song, S. Emerging Hexagonal Mo<sub>2</sub>C Nanosheet with (002) Facet Exposure and Cu Incorporation for Peroxymonosulfate Activation Toward Antibiotic Degradation. *ACS Appl. Mater. Interfaces* **2021**, *13*, 14342–14354. [[CrossRef](#)] [[PubMed](#)]
39. Chen, P.; Liang, Y.; Yang, B.; Jia, F.; Song, S. In Situ Reduction of Au(I) for Efficient Recovery of Gold from Thiosulfate Solution by the 3D MoS<sub>2</sub>/Chitosan Aerogel. *ACS Sustain. Chem. Eng.* **2020**, *8*, 3673–3680. [[CrossRef](#)]
40. Zhu, L.; Ji, J.; Liu, J.; Mine, S.; Matsuoka, M.; Zhang, J.; Xing, M. Designing 3D-MoS<sub>2</sub> Sponge as Excellent Cocatalysts in Advanced Oxidation Processes for Pollutant Control. *Angew. Chem. Int. Ed.* **2020**, *59*, 13968–13976. [[CrossRef](#)]
41. Ji, J.; Aleisa, R.M.; Duan, H.; Zhang, J.; Yin, Y.; Xing, M. Metallic Active Sites on MoO<sub>2</sub>(110) Surface to Catalyze Advanced Oxidation Processes for Efficient Pollutant Removal. *Iscience* **2020**, *23*, 100861. [[CrossRef](#)]
42. Bao, Y.; Chen, T.; Zhu, Z.; Zhang, H.; Qiu, Y.; Yin, D. Mo<sub>2</sub>C/C catalyst as efficient peroxymonosulfate activator for carbamazepine degradation. *Chemosphere* **2022**, *287*, 132047. [[CrossRef](#)]
43. De Andrade, J.R.; Vieira, M.G.A.; Da Silva, M.G.C.; Wang, S. Oxidative degradation of pharmaceutical losartan potassium with N-doped hierarchical porous carbon and peroxymonosulfate. *J. Chem. Eng.* **2020**, *382*, 122971. [[CrossRef](#)]
44. Salazar, C.; Contreras, N.; Mansilla, H.D.; Yáñez, J.; Salazar, R. Electrochemical degradation of the antihypertensive losartan in aqueous medium by electro-oxidation with boron-doped diamond electrode. *J. Hazard. Mater.* **2016**, *319*, 84–92. [[CrossRef](#)] [[PubMed](#)]
45. Guateque-Londoño, J.F.; Serna-Galvis, E.A.; Ávila-Torres, Y.; Torres-Palma, R.A. Degradation of losartan in fresh urine by sonochemical and photochemical advanced oxidation processes. *Water* **2020**, *12*, 3398. [[CrossRef](#)]
46. Martínez-Pach'ón, D.; Espinosa-Barrera, P.; Rinc'on-Ortíz, J.; Moncayo-Lasso, A. Advanced oxidation of antihypertensives losartan and valsartan by photo-electro-Fenton at near-neutral pH using natural organic acids and a dimensional stable anode-gas diffusion electrode (DSA-GDE) system under light emission diode (LED) lighting. *Environ. Sci. Pollut. Res.* **2019**, *26*, 4426–4437. [[CrossRef](#)]
47. Ioannidi, A.; Arvaniti, O.S.; Nika, M.-C.; Aalizadeh, R.; Thomaidis, N.S.; Mantzavinos, D.; Frontistis, Z. Removal of drug losartan in environmental aquatic matrices by heat-activated persulfate: Kinetics, transformation products and synergistic effects. *Chemosphere* **2022**, *287*, 131952. [[CrossRef](#)] [[PubMed](#)]
48. Ioannidi, A.A.; Vakros, J.; Frontistis, Z.; Mantzavinos, D. Tailoring the Biochar Physicochemical Properties Using a Friendly Eco-Method and Its Application on the Oxidation of the Drug Losartan through Persulfate Activation. *Catalysts* **2022**, *12*, 1245. [[CrossRef](#)]
49. García, G.; Guillén-Villafuerte, O.; Rodríguez, J.L.; Arévalo, M.C.; Pastor, E. Electrocatalysis on metal carbide materials. *Int. J. Hydrog. Energy.* **2016**, *41*, 19664–19673. [[CrossRef](#)]
50. Ma, L.; Ting, L.R.L.; Molinari, V.; Giordano, C.; Yeo, B.S. Efficient hydrogen evolution reaction catalyzed by molybdenum carbide and molybdenum nitride nanocatalysts synthesized via the urea glass route. *J. Mater. Chem. A* **2015**, *3*, 8361–8368. [[CrossRef](#)]
51. García, G.; Roca-Ayats, M.; Guillén-Villafuerte, O.; Rodríguez, J.L.; Arévalo, M.C.; Pastor, E. Electrochemical performance of  $\alpha$ -Mo<sub>2</sub>C as catalyst for the hydrogen evolution reaction. *J. Electroanal. Chem.* **2017**, *793*, 235–241. [[CrossRef](#)]
52. Kim, J.; Lee, D.H.; Yang, Y.; Chen, K.; Liu, C.; Kang, J.; Li, O.L. Hybrid Molybdenum Carbide/Heteroatom-Doped Carbon Electrocatalyst for Advanced Oxygen Evolution Reaction in Hydrogen Production. *Catalysts* **2020**, *10*, 1290. [[CrossRef](#)]
53. Han, M.; Wang, H.; Jin, W.; Chu, W.; Xu, Z. The performance and mechanism of iron-mediated chemical oxidation: Advances in hydrogen peroxide, persulfate and percarbonate oxidation. *J. Environ. Sci.* **2023**, *128*, 181–202. [[CrossRef](#)]
54. Lee, C.; Yoon, J. Application of photoactivated periodate to the decolorization of reactive dye: Reaction parameters and mechanism. *J. Photochem. Photobiol., A* **2004**, *165*, 35–41. [[CrossRef](#)]
55. Ioannidi, A.; Frontistis, Z.; Mantzavinos, D. Destruction of propyl paraben by persulfate activated with UV-A light emitting diodes. *J. Environ. Chem. Eng.* **2018**, *6*, 2992–2997. [[CrossRef](#)]
56. Serna-Galvis, E.A.; Botero-Coy, A.M.; Rosero-Moreano, M.; Lee, J.; Hernández, F.; Torres-Palma, R.A. An Initial Approach to the Presence of Pharmaceuticals in Wastewater from Hospitals in Colombia and Their Environmental Risk. *Water* **2022**, *14*, 950. [[CrossRef](#)]
57. Avramiotis, E.; Frontistis, Z.; Manariotis, I.D.; Vakros, J.; Mantzavinos, D. Oxidation of Sulfamethoxazole by Rice Husk Biochar-Activated Persulfate. *Catalysts* **2021**, *11*, 850. [[CrossRef](#)]
58. Tang, H.; Zhao, Y.; Shan, S.; Yang, X.; Liu, D.; Cui, F.; Xing, B. Theoretical insight into the adsorption of aromatic compounds on graphene oxide. *Environ. Sci. Nano* **2018**, *5*, 2357–2367. [[CrossRef](#)]
59. Mrozik, W.; Minofar, B.; Thongsamer, T.; Wiriyaiphong, N.; Khawkomol, S.; Plaimart, J.; Vakros, J.; Karapanagiotti, H.; Vinitantharat, S.; Werner, D. Valorisation of agricultural waste derived biochars in aquaculture to remove organic micropollutants from water—Experimental study and molecular dynamics simulations. *J. Environ. Manag.* **2021**, *300*, 113717. [[CrossRef](#)] [[PubMed](#)]
60. Jawad, A.; Lang, J.; Liao, Z.; Khan, A.; Ifthikar, J.; Lv, Z.; Long, S.; Chen, Z.; Chen, Z. Activation of persulfate by CuO<sub>x</sub>@Co-LDH: A novel heterogeneous system for contaminant degradation with broad pH window and controlled leaching. *J. Chem. Eng.* **2018**, *335*, 548–559. [[CrossRef](#)]
61. Shahzad, A.; Ali, J.; Ifthikar, J.; Aregay, G.G.; Zhu, J.; Chen, Z.; Chen, Z. Non-radical PMS activation by the nanohybrid material with periodic confinement of reduced graphene oxide (rGO) and Cu hydroxides. *J. Hazard. Mater.* **2020**, *392*, 122316. [[CrossRef](#)]

62. Wang, W.; Wang, H.; Li, G.; An, T.; Zhao, H.; Wong, P.K. Catalyst-free activation of persulfate by visible light for water disinfection: Efficiency and mechanisms. *Water Res.* **2019**, *157*, 106–118. [CrossRef]
63. Wang, W.; Wang, H.; Li, G.; Wong, P.K.; An, T. Visible light activation of persulfate by magnetic hydrochar for bacterial inactivation: Efficiency, recyclability and mechanisms. *Water Res.* **2020**, *176*, 115746. [CrossRef]
64. Dong, J.; Shi, Y.; Huang, C.; Wu, Q.; Zeng, T.; Yao, W. A New and stable Mo-Mo<sub>2</sub>C modified g-C<sub>3</sub>N<sub>4</sub> photocatalyst for efficient visible light photocatalytic H<sub>2</sub> production. *Appl. Catal. B.* **2019**, *243*, 27–35. [CrossRef]
65. Cold Spring Harbor Protocols. Available online: [http://cshprotocols.cshlp.org/content/2006/1/pdb.rec8141.full?text\\_only=true](http://cshprotocols.cshlp.org/content/2006/1/pdb.rec8141.full?text_only=true) (accessed on 24 May 2023).
66. Sanders, E.R. Aseptic Laboratory Techniques: Plating Methods. *J. Vis. Exp.* **2012**, *63*, e3064. [CrossRef]
67. Venieri, D.; Karapa, A.; Panagiotopoulou, M.; Gounaki, I. Application of activated persulfate for the inactivation of fecal bacterial indicators in water. *J. Environ. Manage.* **2020**, *261*, 110223. [CrossRef] [PubMed]
68. Lin, K.-Y.A.; Chen, Y.-C.; Lin, Y.-F. LaMO<sub>3</sub> perovskites (M = Co, Cu, Fe and Ni) as heterogeneous catalysts for activating peroxymonosulfate in water. *Chem. Eng. Sci.* **2017**, *160*, 96–105. [CrossRef]
69. Gkika, C.; Petala, A.; Frontistis, Z.; Bampos, G.; Hela, D.; Konstantinou, I.; Mantzavinos, D. Heterogeneous activation of persulfate by lanthanum strontium cobaltite for sulfamethoxazole degradation. *Catal. Today* **2021**, *361*, 130–138. [CrossRef]

**Disclaimer/Publisher’s Note:** The statements, opinions and data contained in all publications are solely those of the individual author(s) and contributor(s) and not of MDPI and/or the editor(s). MDPI and/or the editor(s) disclaim responsibility for any injury to people or property resulting from any ideas, methods, instructions or products referred to in the content.